



Application of a fiber-reinforced copper matrix composite cooling tube to a water-cooled mono-block divertor component: A design study

J.H. You *

Max-Planck-Institut für Plasmaphysik, Euratom Association, Boltzmannstr. 2, 85748 Garching, Germany

A B S T R A C T

Fiber-reinforced copper matrix composites are considered as a promising heat sink material for future divertor. In this article the structural reliability of a water-cooled tungsten mono-block divertor component with a composite cooling tube is treated. An integrated modeling scheme for multi-scale failure analysis is presented. The applied micromechanics-based FEM technique could be successfully combined with various failure analysis models to predict the failure risk on different length scales. It was demonstrated that the composite divertor component is a reasonable design concept in terms of structural reliability.

© 2009 Elsevier B.V. All rights reserved.

1. Introduction

Fiber-reinforced copper matrix composites (FCMC) are considered as a promising heat sink material for future divertor [1]. Their advantage is the combination of high thermal conductivity of the copper alloy matrix with excellent high-temperature strength of the strong fibers [2]. In this article the structural reliability of a water-cooled tungsten mono-block divertor component with a FCMC cooling tube is treated. The FCMC cooling tube was assumed to be reinforced with continuous tungsten fibers in the tube hoop direction.

The structural reliability of the FCMC tube will be essentially affected by the micro-scale failures such as fiber fracture or matrix damage. These micro-scale failures are directly governed by the micro-scale stress and strain. To estimate these quantities, a micromechanics-based dual-scale finite element method (FEM) was applied [3]. There are also further failure features which can be better assessed on higher length scales. If a thermal stress fluctuation is generated, the FCMC cooling tube may show either shakedown or alternating plasticity. In this regard, shakedown boundary is the proper failure criterion. The FCMC tube eventually reaches safe elastic state under a varying load, provided that the peak load is bounded within the shakedown boundary [4]. These plastic responses are most suitably described on a mesoscopic length scale. Brittle failure is a crucial issue for the tungsten component due to its inherent brittleness. Being subjected to neutron irradiation, tungsten is further embrittled [5]. Therefore, a fracture mechanical failure analysis is necessary to assess the macro-scale

failure risk. Scattering of the strength data requires a statistical approach.

In this work, multi-scale failure analysis was carried out to estimate the failure risks of the divertor composite component on three different length scales.

2. FEM model and loading condition

The reference model was the water-cooled tungsten mono-block divertor designed for the WCLL reactor [6]. In the present study the original cooling tube material (copper alloy) was replaced with a FCMC. The model geometry (symmetric half) and the FEM mesh (10400 elements) are shown in Fig. 1. The dimension was $19.5 \times 18 \times 4 \text{ mm}^3$. The cooling tube had inner diameter of 10 mm and thickness of 2 mm. The considered FCMC was a unidirectional lamina consisting of copper alloy matrix reinforced with continuous tungsten fibers (fiber volume fraction: 40%). Material properties are listed in Table 1 [7].

At first, residual stresses were generated assuming a uniform cooling from the stress-free temperature 500 °C to room temperature. Subsequently, thermal loading was simulated assuming a heat flux load of 15 MW/m² and coolant temperature of 320 °C. The heat transfer coefficient was 0.156 MW/m² K.

3. Computational scheme

3.1. Micromechanics model

In the non-linear dual-scale FEM, stresses and strains are computed on the micro- and on the macro-scale simultaneously. A material law based on the incremental mean field theory was used. The material subroutine algorithm of Pettermann was applied for

* Tel.: +49 89 3299 1373.
E-mail address: you@ipp.mpg.de

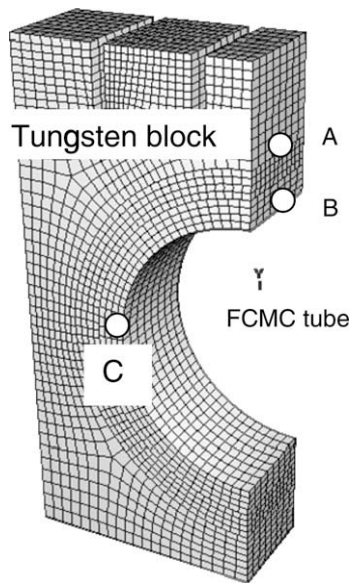


Fig. 1. Geometry (symmetric half) and the finite element mesh of the model composite component consisting of tungsten armor block and FCMC heat sink cooling tube. FCMC was a unidirectional composite consisting of copper alloy matrix reinforced with tungsten fibers wound in the tube hoop direction (fiber volume fraction: 40%).

the implementation into a FEM code [8]. Each composite element consisted of four unidirectional fiber layers.

3.2. Direct shakedown analysis

The shakedown boundary of the FCMC was obtained using the FEM-based direct shakedown analysis method developed by Weichert [4] which was based on the Melan's shakedown theorem. In this method, the shakedown conditions are checked at individual Gauss integration points for which a large-scale non-linear optimization problem has to be solved. The shakedown boundary of the FCMC tube was computed for the bi-axial loading state appearing at the cooling tube wall [9].

3.3. Probabilistic failure analysis

For the analysis of brittle failure a FEM-based probabilistic failure analysis code STAU was used [10]. In STAU the probabilistic failure description was based on the weakest-link failure theory, Weibull statistics and fracture mechanics. Four different mixed-mode fracture criteria were considered. The Weibull parameters of tungsten strength were measured. The estimated Weibull modulus was 30 and the scale parameter amounted 2350 MPa.

Table 1
Selected material properties used for the FEM simulation [7].

	Tungsten block ^a	CuCrZr matrix	W wire ^b
Young's modulus (GPa)	400 (20 °C)	128 (20 °C)	400 (20 °C)
	393 (400 °C)	110 (400 °C)	393 (400 °C)
Yield stress (MPa)	1385 (20 °C)	300 (20 °C)	2000 (20 °C)
	950 (400 °C)	273 (400 °C)	
Heat conductivity (W/mK)	175 (20 °C)	380 (20 °C)	175 (20 °C)
	140 (400 °C)	350 (400 °C)	140 (400 °C)
CTE (10 ⁻⁶ /K)	4.5 (20 °C)	15.7 (20 °C)	4.5 (20 °C)
	4.6 (400 °C)	19.3 (400 °C)	4.6 (400 °C)

^a Cold worked and annealed (stress relieved) tungsten.

^b Measured by tensile test using laser speckle strain gauge.

4. Results and discussion

4.1. Thermal response

The steady state surface temperature ranged from 984 °C to 1204 °C. The maximum temperature of the cooling tube was 536 °C at the upper bond interface and 443 °C at the inner wall.

4.2. Evaluation of fiber failure risk by micromechanics analysis

In Fig. 2, the tungsten fiber stresses at the upper position of the tube are shown for the residual stress state at room temperature and for the heat flux loading stage. Stress profiles are plotted along a radial path in the thickness direction toward the tube wall (path AB in Fig. 1).

The fibers experienced significant stress relaxation upon heat flux loading. This stress reduction was ascribed to the increased tube temperature approaching the stress-free temperature.

The peak tensile stress appearing at the tube wall reached 2385 MPa. This value amounts to 80–90% of the tensile strength of tungsten wires (2.7–3.0 GPa).

Before the fusion operation tungsten wires experience no embrittlement. In the unirradiated state, tungsten wires exhibit a notable ductility with a large Weibull modulus larger than 200 indicating a small scattering of the strength. Fully elasto-plastic FEM sub-modeling analysis revealed that significant fiber stress relaxation occurred up to 40% due to the plastic yield.

During the heat flux loading the fiber stress was markedly relieved. The maximum tensile fiber stress appearing at the upper tube wall reached only 1560 MPa. Although the tungsten fibers are embrittled by irradiation during the heat flux loading, the fibers will not fail because the maximum stress amounts only 60% of the fiber strength.

4.3. Evaluation of matrix damage

A significant plastic straining occurred in the FMMC matrix upon the heat flux loading which could cause damage. For a quantitative assessment of the matrix damage a damage indicator defined by Rice and Tracey was estimated [8]. This damage parameter was so calibrated that the critical value of unity would correspond to the onset of local failure by micro-crack initiation. The

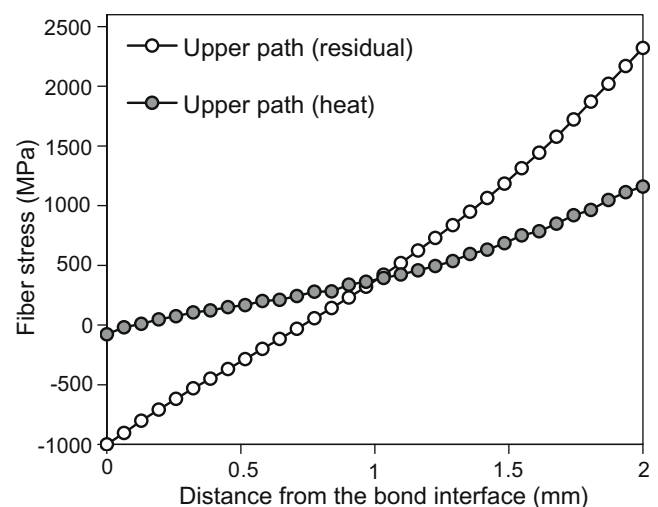


Fig. 2. Profiles of the micro-scale tungsten fiber stress (axial component). Results are estimated for the residual stress state and for the heat flux loading state. The abscissa denotes the positions along the upper path (path AB) of the tube in radial direction starting from the bond interface toward the tube wall.

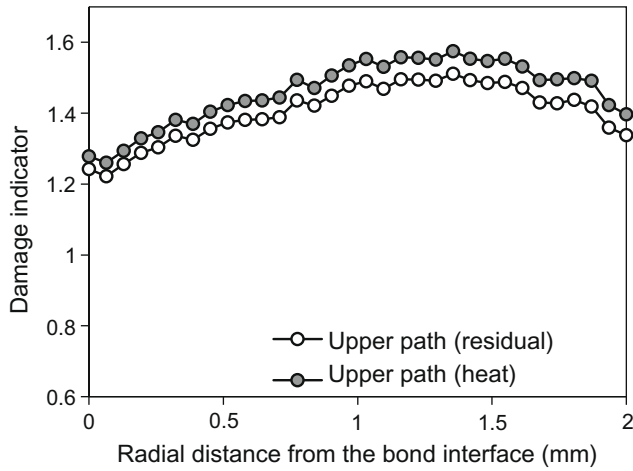


Fig. 3. Profiles of the estimated damage indicator defined by Rice and Tracey. Results are estimated for the residual stress state and for the heat flux loading state. The abscissa denotes the positions along the upper path (path AB) of the tube in radial direction starting from the bond interface toward the tube wall.

profiles of the damage indicator are plotted in Fig. 3. The damage indicator exceeded the critical value already before the thermal loading. This early development of damage can be attributed to the tensile hydrostatic stress dominating in the FCMC matrix during the fabrication. Upon the heat flux loading, the damage indicator increased only slightly. This positive behavior was ascribed to the hydrostatic compression of the matrix during the thermal loading. The damage level seems to be acceptable.

4.4. Results of shakedown analysis

To evaluate the plastic failure risk of the FCMC tube, the meso-scale composite tube stresses were compared with the shakedown boundary of the FCMC. The meso-scale stresses were obtained from the micromechanical homogenization procedure in which the micro-scale stresses were averaged over each fiber layer in a composite element.

The most critical region was the upper tube wall where the tube hoop stress reached the maximum value. The tube wall region was loaded in a plane stress state. In Fig. 4, the stress states at the upper

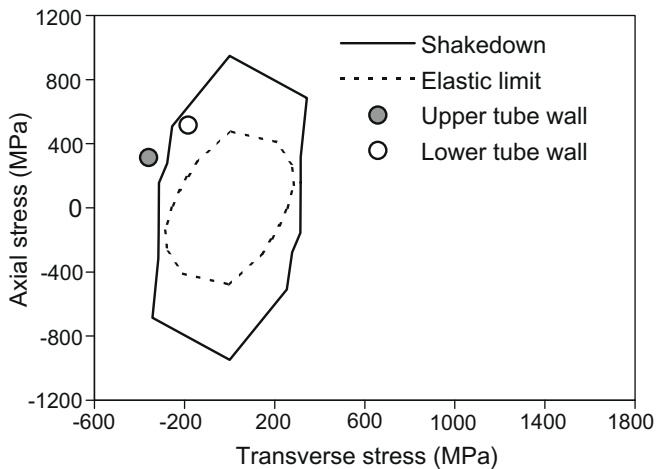


Fig. 4. Meso-scale lamina stress states under heat flux loading at two tube wall positions (position B and C) compared with the computed shakedown boundary of the tungsten fiber-reinforced copper alloy matrix composite (unidirectional lamina).

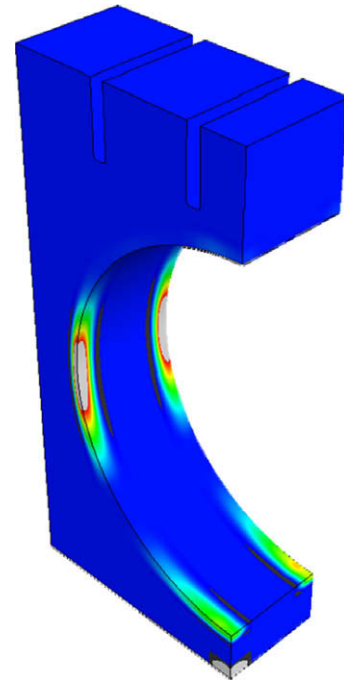


Fig. 5. Distribution of local risk of fracture illustrated in an arbitrary colour scale. (For interpretation of the references to colour in this figure legend, the reader is referred to the web version of this article.)

Table 2
Failure probabilities under heat flux loading.

Shape parameter	Scale parameter	Fracture criteria	Failure probability (%)
31	2353	Coplanar G	0.0085
		Normal stress	0.0169
		Hoop stress	0.0068
		Max. G	0.0065

and middle tube wall position (position B and C) are compared with the computed shakedown boundary of the FCMC. The tube wall stresses were located very close to the shakedown boundary which indicates that the risk of plastic failure at the tube wall is low.

4.5. Results of probabilistic failure analysis

The distribution of local risk of fracture (failure probability density) during the heat flux loading is presented in Fig. 5 in an arbitrary colour scale. The highest risk of local fracture appeared near the free surface edges of the bond interfaces between the tungsten block and the cooling tube where the stress concentration appeared as well.

The estimated failure probabilities of the tungsten block are summarized in Table 2. The four fracture criteria predicted a little different results. The largest failure probability was only 0.017%.

It was also found that the failure probability of the tungsten block was strongly reduced through the FCMC reinforcement of the tube.

5. Conclusions

In this work an integrated modeling scheme of multi-scale failure analysis was presented for a water-cooled mono-block divertor

component reinforced with a fiber composite cooling tube. The applied micromechanics-based FEM technique could be successfully combined with various failure analysis models to predict the failure risk of the composite component on different length scales. It was demonstrated that the composite divertor component is a reasonable design concept in terms of the structural reliability.

References

- [1] A. Brendel, C. Popescu, T. Köck, H. Bolt, J. Nucl. Mater., 367–370 (2007) 1476.
- [2] J.H. You, H. Bolt, J. Nucl. Mater. 305 (2002) 14.
- [3] J.H. You, J. Nucl. Mater. 336 (2005) 97.
- [4] D. Weichert, A. Hachemi, F. Schwabe, Arch. Appl. Mech. 69 (1999) 623.
- [5] N. Baluc, Assessment Report on W, Final Report on EFDA Task TW1-TTMA-002 Deliverable 5, 2002.
- [6] A conceptual study of commercial fusion power plants, Final Report of the European Fusion Power Plant Conceptual Study (PPCS) EFDA-RP-RE-5.0, 2004.
- [7] ITER Material Properties Handbook (IMPH), ITER Document No. S74 RE1 and G74 MA16, 2005.
- [8] H.E. Pettermann, A.F. Plankensteiner, H.J. Böhm, F.G. Rammerstorfer, Comput. Struct. 71 (1999) 197.
- [9] J.-H. You, B.Y. Kim, M. Miskiewicz, Mech. Mater., in press, doi: 10.1016/j.mechmat.2008.10.007.
- [10] A. Brückner-Foit, A. Heger, K. Heiermann, P. Hülsmeier, A. Mahler, A. Mann, Ch. Ziegler, STAU 4 User's Manual, Forschungszentrum Karlsruhe, Karlsruhe, 2003.